JCTC Journal of Chemical Theory and Computation

Calculation of Quasi-Particle Energies of Aromatic Self-Assembled Monolayers on Au(111)

Yan Li,* Deyu Lu, and Giulia Galli

Chemistry Department, University of California, Davis, California 95616

Received October 31, 2008

Abstract: We present many-body perturbation theory calculations of the electronic properties of phenylene diisocyanide self-assembled monolayers (SAMs) on a gold surface. Using structural models obtained within density functional theory (DFT), we have investigated how the SAM molecular energies are modified by self-energy corrections and how they are affected by the presence of the surface. We have employed a combination of GW (G = Green's function; W = screened Coulomb interaction) calculations of the SAM quasi-particle energies and a semiclassical image potential model to account for surface polarization effects. We find that it is essential to include both quasi-particle corrections and surface screening in order to provide a reasonable estimate of the energy level alignment at a SAM−metal interface. In particular, our results show that within the GW approximation the energy distance between phenylene diisocyanide SAM energy levels and the gold surface Fermi level is much larger than that found within DFT, e.g., more than double in the case of low packing densities of the SAM.

1. Introduction

The study of the self-assembly of molecular monolayers of materials and their applications for electronic and optical devices has been an active field of research for the past 2 decades.[1] In particular, aromatic self-assembled monolayers (SAMs) have been proposed to be promising candidates for electron-transport applications because of the delocalized nature of their π electrons and the relatively small energy gap between the highest occupied molecular orbital (HOMO) and the lowest unoccupied molecular orbital (LUMO), which may give rise to low barriers for electron or hole transport. In order to predict such barriers and thus the performance of SAM−metal devices, it is essential to understand, at the microscopic level, the structural and electronic properties of the molecule−electrode interfaces.

Density functional theory (DFT) has been widely used to study these properties, and usually the structure and energetics of SAM−metal interfaces are reasonably well described, as compared, e.g., to experimental findings. On the other hand, the deficiencies of DFT in describing energy levels in small molecules are well-known: the Kohn−Sham energy eigenvalues are usually not a good representation of molecular orbital energies, and the predicted HOMO−LUMO gap is in most cases underestimated with respect to the experimentally measured difference of electron removal and addition energies. As a consequence, the conductance of electrons or holes estimated using $|E_F - E_{HOMO}|$ or $|E_F - E_{LUMO}|$ is often seriously overestimated (E_F is the Fermi level). Moreover, the electrostatic polarization from the metal substrate, partly missing in conventional DFT calculations, may also significantly affect the values of electron removal and addition energies. For example, it was recently reported that the computed conductance of single-molecule benzenediamine−gold junctions as obtained within DFT is about 7 times larger than that in experiment[2] and the self-energy correction and surface polarization effect were estimated to shift the HOMO level by −3 and +1 eV, respectively.

In order to gain insight into the alignment of SAM−metal energy levels beyond semilocal DFT approximations, we have carried out calculations of SAM quasi-particle energies using many-body perturbation theory within the GW approximation (G = Green's function; W = screened Coulomb interaction). We have also included surface polarization effects by using a semiclassical image potential model, which was proposed and successfully employed in several recent studies of organics−metal interfaces or

* Corresponding author e-mail: ynli@ucdavis.edu.

10.1021/ct800465f CCC: $40.75
Published on Web 01/09/2009

junctions.[2,3] In particular, we have studied SAMs of 1,4-phenylene diisocyanide (PDI) on Au(111), and we have considered different surface coverages. The energetic, electronic, and vibrational properties of PDI SAMs adsorbed on the Au(111) surface have been reported in an earlier work,[4] and here we use the structural model determined in ref 4 to investigate the energy level alignment at the interface.

It has been suggested that aromatic isocyanides may have promising transport properties: the presence of a triple bond in the isocyanide group (−NC) may effectively connect pπ orbitals residing on the aromatic moiety and the dπ orbitals pointing out of the gold surface, thus providing a good network of delocalized electrons and thereby lowering the barrier for charge injection from the metal into the organic semiconductor.[5] However, no consensus has been reached about the performance of such systems from electrical conductivity measurements.[6−11] For example, the study of Chu et al. on the conductance of alkanes and biphenyl- and diphenylacetylene bridges with thiol and isocyanide terminals suggested that the conductivity is enhanced by an order of magnitude when the thiol−gold linkage is replaced with an isocyanide−gold linkage,[11] while the opposite trend was reported by other groups.[10]

Most of the existing theoretical investigations of transport properties of isocyanide molecules have been based on DFT in the local density (LDA) or generalized-gradient-corrected (GGA) approximations and on nonequilibrium Green function calculations.[12,13] One of these studies[12] reported that in a system comprising a single PDI molecule sandwiched between two gold electrodes the gold Fermi level (E_F) is in near-resonance with the delocalized LUMO state of the PDI molecule, leading to a large zero-bias conductance (45.8 μS) that is much higher than that of benzenedithiol (4.8 μS) calculated using the same method.[14] Similarly, a moderate electron barrier $|E_{LUMO} - E_F| \sim 0.7$ eV was obtained within DFT for the low-density PDI SAM adsorbed on the Au(111) surface.[4] These predictions appear to be consistent with the experimental findings of Chu et al.[11] However, as was already mentioned, transport calculations using energy levels obtained using DFT within LDA or GGA usually overestimate conductance values, because they underestimate energy barriers for charge transport.[15,16] Therefore, it is important to explore ways to obtain the relative position of the SAM and metal surface energy levels, beyond local and semilocal DFT approximations.

The rest of the paper is organized as follows: in section 2, we describe the method and geometrical models used in our calculation. In section 3, we present the GW self-energy calculations and compare them to the DFT results. In section 4, we describe the semiclassical model for the polarization effect from the metal substrate. Section 5 concludes the paper.

2. Methods

Because of the complexity and large computational cost of quasi-particle energy calculations of a system comprising a SAM and a metal, we have split our calculation into two parts: the self-energy corrections for a free-standing PDI SAM were first obtained through a GW self-energy calculation, and we assume that this correction term remains the same after the slight structural relaxation of the SAM upon adsorption on the metal surface. Surface polarization effects were then included as an external perturbation to the orbitals of the adsorbed SAM through a semiclassical image potential model.

The free-standing PDI SAMs were arranged in $(\sqrt{3} \times \sqrt{3})$ or (3×3) unit cells, which correspond to high ($\Theta = 1$) and low coverage ($\Theta = {}^1/_3$), respectively. The nearest-neighbor distances, d_{NN}, are 5.10 and 8.83 Å for the two packing densities, assuming a lattice constant of 4.16 Å for the underlying Au(111) surface in the adsorbate system, as determined from DFT calculations for bulk gold.[4] The two-dimensional periodic SAM was then placed in a supercell with a 10 Å vacuum separation between SAMs in neighboring supercells in the self-consistent ground-state calculations. The Brillouin zone was sampled with a $6 \times 6 \times 1$ Monkhorst−Park grid of k points for high coverage and a $3 \times 3 \times 1$ grid for the low-coverage structure. The SAM band structures were generated by non-self-consistent calculations along the edges of the irreducible Brillouin zone.

Both DFT and GW calculations were performed using the ABINIT code.[17,18] Geometries of the free-standing PDI SAMs were first fully relaxed, and their ground-state properties were evaluated by performing plane-wave pseudopotential calculations within DFT, in the Perdew−Burke−Ernzerhof (PBE) GGA.[19] We employed norm-conserving pseudopotentials generated with the PBE exchange and correlation functionals, and details can be found in ref 4. Wave functions were expanded in plane waves with an energy cutoff of 50 Ry. DFT energy eigenvalues and wave functions were then used to construct the inverse dielectric matrix $\varepsilon_{G,G'}^{-1}$ (G and G' indicate the reciprocal lattice vectors) and evaluate the self-energy operator Σ in the GW approximation. The frequency dependence of the dielectric matrix was approximated by the plasmon-pole model (PPM) proposed by Godby and Needs.[20] The self-energy correction for orbital i was then estimated as $\Delta E_i = \langle \Psi_i | \Sigma - V_{xc} | \Psi_i \rangle$, where V_{xc} is the DFT exchange-correlation (xc) potential and $|\Psi_i\rangle$ is the DFT wave function of orbital i. In the high-coverage case ($\Theta = 1$), the matrix elements of the self-energy operator were evaluated with a 25 Ry energy cutoff for the exchange part Σ_x and a 15 Ry energy cutoff for the correlation part Σ_c; a total of 400 conduction bands (~60 eV above E_{HOMO}) were included. In the low-coverage case ($\Theta = {}^1/_3$), a 25 Ry cutoff for Σ_x, a 10 Ry cutoff for Σ_c, and 700 conduction bands (~45 eV above E_{HOMO}) were used. Further increasing the energy cutoffs or the number of conduction bands has little influence on the magnitude of the quasi-particle gap, while both HOMO and LUMO are slightly shifted to lower energies.

For finite (nonperiodic) systems, one needs to eliminate spurious interactions between different supercells, when one evaluates the electron removal and addition energies. In order to do so in our GW calculations, we used the two-dimensional Coulomb cutoff technique proposed in ref 21, For high-density PDI SAMs, the differences between quasi-particle energies computed with or without a Coulomb cutoff are on the order of 0.1−0.2 eV.

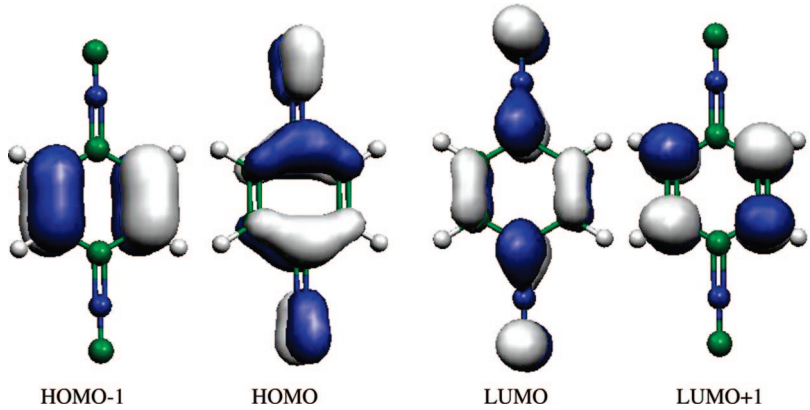

Figure 1. Isosurface plots of HOMO−1, HOMO, LUMO, and LUMO+1 states of the PDI molecule in the gas phase, as obtained within DFT/PBE. The corresponding orbital energies are −7.6, −6.9, −3.1, and −2.5 eV, from left to right.

3. Quasi-Particle Energies of PDI SAMs

The PDI molecule contains an aromatic ring and two isocyanide groups. The molecular orbitals can be separated into two groups: those derived from the benzene molecular orbitals and those mainly localized on the isocyanide groups. The HOMO−1, HOMO, LUMO, and LUMO+1 states of gas-phase PDI and the corresponding DFT orbital energies are shown in Figure 1: these are derived from the doubly degenerate HOMOs and LUMOs of benzene. The degeneracy present in benzene is now lifted in the HOMO and LUMO of the PDI molecule, defined as π_P and π_P^*; the π orbitals on the benzene ring couple to those on the isocyanide groups, and their energy levels are drawn closer, with a gap of 3.8 eV. At the same time, the HOMO−1 and LUMO+1 states remain the same as those in benzene, and they are thus defined as π_B and π_B^*. The energy difference between π_B and π_B^* (∼5.1 eV) is close to the corresponding one of the benzene molecule computed within DFT.[3] The GW quasi-particle gap of gas-phase benzene is estimated to be about 10.5 eV, i.e., ΔE_g ($=E_g^{GW} - E_g^{DFT}$) ∼ 5 eV, and one expects a similar ΔE_g for gas-phase PDI. Indeed, the total energy differences of the neutral molecule and corresponding cation−anion yield $E_{HOMO} = -9.5$ eV and $E_{LUMO} = -0.9$ eV ($E_g = 8.6$ eV). These energy levels were obtained using *Gaussian03*,[22] DFT/PBE with a aug-cc-pvTZ basis set.

When PDI molecules are arranged into a periodic SAM structure, the molecular energy levels broaden and shift with respect to those of the isolated molecule because of intermolecular interactions within the SAM. Figure 2a plots the DFT band structure of the (3 × 3) PDI SAM. The occupied bands are nearly dispersionless and so are the lower unoccupied bands. Other bands higher in energies show moderate dispersion. In contrast, for the ($\sqrt{3} \times \sqrt{3}$) high-density SAM (Figure 2b), the dispersion within the bands becomes more pronounced. In addition, the energy bands are found to shift down by about 1 eV relative to those of the low-density SAM. This is caused by the local charge polarization effect between the aromatic moiety and the two isocyanide groups because of the strong acceptor nature of the latter. At high density, the molecules experience a deeper potential well formed by the two local dipole layers at the SAM edges, and therefore the energy levels shift down with respect to the vacuum level. For the same reason, π_B and π_B^* are located at lower energy in PDI than in benzene, even in the gas phase. An opposite trend is found when the −NC group is replaced by the $-NH_2$ group, which is a strong electron donor.

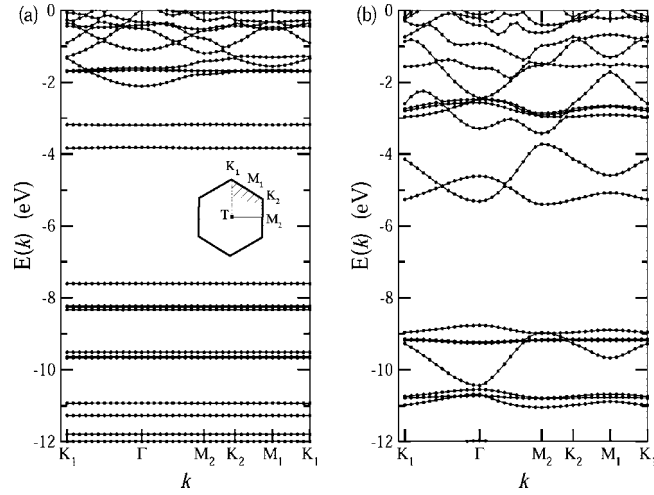

Figure 2. DFT/PBE band structure of PDI SAMs at low and high packing densities (see the text). Inset: irreducible Brillouin zone in the *x*−*y* plane. All energies have been adjusted to the vacuum energy level.

Next, we calculate the GW self-energy corrections to the DFT energy bands. At low coverage, because the bands are mostly dispersionless, the corrections are expected to be similar at different *k* points. Indeed, the GW corrections at, for example, Γ and *K* differ by only a few tens of millielectronvolts. Table 1 shows the DFT Kohn−Sham orbital energies E^{DFT} and GW quasi-particle energies E^{GW} at Γ = (0, 0, 0). The states labeled as $\sigma_\pm$ correspond to σ orbitals localized on the isocyanide groups with even or odd horizontal mirror symmetry, respectively. Although DFT energies of $\sigma_\pm$ states are nearly degenerate with that of the π_B state, self-energy corrections are larger for these localized states and the GW quasi-particle energies turned out to be about 0.6 eV below that of π_B. All energies here have been adjusted relative to the vacuum energy level, which is taken as the plane-averaged Hartree potential (containing both electronic and ionic contributions) in the middle of the vacuum region.

Table 1. DFT/PBE Single-Particle Energies and GW Quasi-Particle Energies (in eV) of Orbitals of the (3 × 3) PDI SAM Structure at the Γ Point[a]

	E^{DFT}	V_{xc}^{DFT}	Σ_x	$\Sigma_c(E^{DFT})$	ΔE	E^{GW}
π_B	−8.34	−13.06	−15.57	0.67	−1.50	−9.84
σ_+	−8.27	−13.58	−18.68	2.21	−2.20	−10.47
σ_-	−8.23	−13.65	−18.71	2.20	−2.19	−10.42
π_P	−7.60	−13.98	−16.00	0.33	−1.40	−9.01
π_P^*	−3.81	−13.09	−8.31	−1.13	3.06	−0.75
π_B^*	−3.19	−12.49	−7.45	−1.48	2.98	−0.21

[a] V_{xc}^{DFT}, Σ_x, and $\Sigma_c(E^{DFT})$ correspond to the expectation values of the DFT xc potential and the exchange and correlation parts (evaluated with DFT energies) of the self-energy operator, respectively. $E^{GW} = E^{DFT} + \Delta E = E^{DFT} + [\Sigma(E^{GW}) - V_{xc}^{DFT}]$, in which $\Sigma(E^{GW})$ is obtained from Σ_x and $\Sigma_c(E^{DFT})$ by linear expansion.

A few observations from Table 1: first, the energy levels of occupied states shift down and those of unoccupied state shift up when GW corrections are added to the DFT eigenvalues. This shift is not symmetric. For example, the energies of the π_P and π_B orbitals are shifted by −1.50 and −1.40 eV, while those of the π_P^* and π_B^* orbitals are shifted by 3.06 and 2.98 eV, respectively. Second, self-energy corrections are strongly dependent on the localization of the single-particle wave functions. For more localized states such as $\sigma_\pm$, the correction is about 0.7 eV larger than that for delocalized π_P and π_B states. Third, the quasi-particle gap is 8.3 eV, much larger than the DFT/PBE, HOMO−LUMO gap, but it is still smaller than the quasi-particle gap of the gas-phase PDI molecule (8.6 eV). The energy distance between π_B and π_B^* also increases from 5.1 to 9.6 eV, and it is close to that of the gas-phase benzene molecule (10.5 eV) estimated within GW.[3] The fact that the energy separations are smaller in the SAM than in the isolated molecule indicates that even at low density there exists a weak screening within the SAM that reduces the separation between HOMO and LUMO, in comparison with the case of an isolated molecule.

Similarly, one expects the GW gap of SAMs to further decrease as the packing density increases. This is indeed the case for the high-density SAM, as shown in Table 2. Self-energy corrections are presented at different k points: Γ, K_1, and M_2. One finds that although the dispersion of the DFT bands can be as large as 1−1.5 eV (see also Figure 2b) the GW corrections (ΔE) for different k points amount to a shift that is almost rigid. The vertical gaps between π_P and π_P^* are 7.9, 7.3, and 7.2 eV at the three k points shown in Table 2, obviously smaller than the corresponding values at low packing density.

Although a direct comparison with the experiment is not available for the energy levels of the PDI molecule and PDI SAM, we can estimate possible inaccuracies of our GW approach by comparing it with the experimental results obtained for the benzene molecule. We carried out quasi-particle calculations for benzene using a face-centered-cubic supercell of lattice constant $a = 18.5$ Å. Electronic wave functions were obtained from DFT/LDA ground-state calculations and expanded in plane waves with an energy cutoff of 50 Ry. GW corrections were evaluated with energy cutoffs of 20 and 10 Ry for the exchange and correlation parts, respectively, and with a total of 1000 conduction bands (∼50 eV above E_{HOMO}). Using the PPM by Godby and Needs, we found quasi-particle energies of the HOMO (−8.35 eV) and LUMO (1.85 eV) levels of benzene in good agreement with those obtained by Niehaus et al., who carried out GW calculations with Gaussian-type orbitals.[23] However, both energies are shifted by about 1 eV compared with values obtained from experiments[24,25] and by doing total energy differences within LDA. There are several factors contributing to this energy shift: (1) As mentioned earlier in section 2, we found that the GW-corrected orbital energies always shift downward when one increases the plane-wave energy cutoff for the self-energy operator or includes more conduction bands for the dielectric matrix calculation. The convergence on the latter was found to be rather slow. The asymptotic limit of the quasi-particle energies was obtained by varying the energy cutoff of the sum over conduction bands measured from the HOMO level (defined as E_c), similar to the procedure of Umari et al.[26] By extrapolating the GW corrections to $E_c \rightarrow \infty$, we found $E_{HOMO}^{\infty} = -8.65$ eV and $E_{LUMO}^{\infty} = 1.46$ eV. (2) Another possible source of error is the use of a PPM instead of explicit energy integration over the frequency dependence of the dielectric function. It has been demonstrated earlier that GW calculations with PPM yield reasonable results for the ionization potential and electron affinity of selected isolated systems.[27] Yet, the influence of PPM on aromatic systems such as PDI SAMs is not clear. Furthermore, we found that that using different PPMs such as those proposed by Godby and Needs[20] and by von der Linden and Horsch,[28] the GW energy corrections can differ by about 0.3−0.4 eV. (3) Additional corrections may be obtained by performing self-consistent GW calculation and/or by going beyond the random-phase approximation for the dielectric matrix. For the sake of completeness, we note that the GW results on the benzene molecule reported by Tiago and Chelikowsky[29] are in good agreement with experiment. Several numerical approximations different from those used here were adopted in ref 29, and the origin of the discrepancy between our and ref 23 results and Tiago and Chelikowsky's results is not fully understood. Overall, it is not unreasonable to expect that the position of the HOMO and LUMO levels of the PDI molecule and of the SAMs computed here may be rigidly shifted upward with respect to experiment by approximately the same amount.

In summary, we found that through application of GW self-energy corrections to the Kohn−Sham energy levels of PDI SAM structures the HOMO−LUMO gap is significantly increased, with the occupied and unoccupied bands shifted in opposite directions. The magnitude of the shift depends on the localization of the orbitals, but it only varies slightly within the same band. At high packing density, screening among neighboring molecules decreases the HOMO−LUMO gap by about 1 eV. Because it was found that low coverage of PDI SAM is energetically more favorable on the Au(111) surface,[4] we will focus on the (3 × 3) structure in the following and apply the GW energy corrections computed above to the adsorbed SAM structure. However, before doing so, we discuss the surface polarization in the next section.

Table 2. DFT/PBE and GW Energies (in eV) of Orbitals of the ($\sqrt{3} \times \sqrt{3}$) PDI SAM Structure at Three Different *k* Points

	$\Gamma = (0, 0, 0)$			$K_1 = (1/3, 1/3, 0)$				$M_2 = (1/2, -1/2, 0)$			
	E^{DFT}	ΔE	E^{GW}		E^{DFT}	ΔE	E^{GW}		E^{DFT}	ΔE	E^{GW}
π_B	−10.44	−1.36	−11.80	π_B	−9.27	−1.12	−10.39	σ_+	−9.19	−2.06	−11.24
σ_+	−9.26	−2.08	−11.34	σ_+	−9.18	−2.06	−11.23	σ_-	−9.16	−2.04	−11.20
σ_-	−9.23	−2.06	−11.29	σ_-	−9.15	−2.04	−11.19	π_P	−8.99	−1.23	−10.21
π_P	−8.76	−1.16	−9.92	π_P	−8.96	−1.22	−10.18	π_B	−8.96	−1.05	−10.01
π_B^*	−5.31	2.17	−3.14	π_P^*	−5.26	2.38	−2.88	π_P^*	−5.39	2.34	−3.06
π_P^*	−4.61	2.60	−2.00	π_B^*	−4.14	2.41	−1.73	π_B^*	−3.72	2.53	−1.19

4. Polarization from the Metal Substrate

It is well-known that in DFT the xc potential within local or semilocal approximations fails to reproduce the asymptotic image potential tail shape of a metal surface.[30,31] Long-range many-body effects, absent in most conventional DFT approximations, are expected to screen the Coulomb potential experienced by an added hole or electron and thus effectively decrease the HOMO−LUMO gap of the isolated SAM. In principle, this effect can be captured by performing GW calculations for the whole SAM-on-metal system (see, e.g., ref 3). Because of the complexity and huge computational cost to carry out such calculations on a large metallic system, here we adopt a semiempirical treatment. To account for this polarization effect from the metal substrate, we add the following correction term to the quasi-particle energy level $E^{GW}(j)$ calculated for a given SAM molecular orbital j:

$$\Delta P^{surface}(j) = \int_{z>z_1} dr\, [V_{im}(r) - V_{xc}^{Au(111)}(r)]\rho_j^{SAM}(r) \quad (1)$$

$$V_{im}(r) = -\frac{e^2}{4|z - z_0|} \quad (2)$$

where $V_{im}(r)$ and $V_{xc}^{Au(111)}(r)$ are the image potential and the DFT xc potential of a clean Au(111) surface, respectively; $\rho_j^{SAM}(r)$ is the electron density of orbital j of the SAM. To evaluate $V_{xc}^{Au(111)}$ and ρ_j^{SAM}, DFT calculations were carried out separately for the two subsystems, adopting the atomic positions determined in the optimized SAM−Au(111) system.[4] z_0 is the image plane position, and z_1 is the where $V_{xc}^{Au(111)}(r)$ starts to deviate from the effective local quasi-particle xc potential, assuming that the latter crosses smoothly from $V_{xc}^{Au(111)}(r)$ to $V_{im}(r)$ at z_1. z_0 and z_1 were therefore determined by computing the intersection of the plane-averaged potentials $V_{xc}^{Au(111)}(z)$ and $V_{im}(z)$, as shown in Figure 3. This approximation is consistent with GW calculations for Al surfaces;[30,31] our fitted mirror-plane position is about 1.0 Å above the first layer of gold atoms, which compares well with the corresponding values adopted for graphite[3] and gold[2] surfaces in similar instances.

We note that in order to treat surface polarization effects as an external perturbation the adsorbate orbitals are required to be well separated from the metal substrate. This is true, for example, in the case of benzene molecules physisorbed on the graphite surface.[3] Although the PDI molecules are chemisorbed on Au(111), with a binding energy of about 0.5 eV,[4] the LUMO-like adsorbate orbitals are found to be only weakly coupled to the metal surface. Indeed, for these states, approximately 90% of the wave function is localized on the SAM itself. Therefore, the use of eq 1 is justified. By

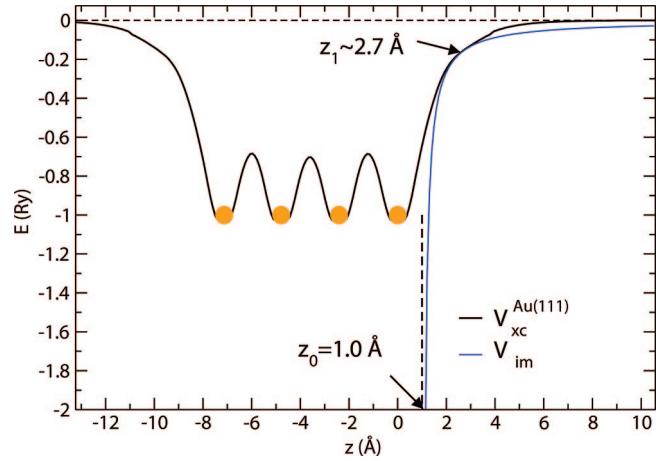

Figure 3. Plane-averaged DFT/PBE xc potential (V_{xc}) calculated from a clean Au(111) slab and a classical image potential $V_{im} = -1/4|z - z_0|$. The origin is set at the first layer of gold atoms, and z_0 and z_1 were fitted by setting the intersection of the two curves at z_1.

application of the correction in eq 1, the energy levels of LUMO-like states are lowered by about 0.5 eV. When this term is combined with the self-energy correction obtained for the isolated SAM, the LUMO level is predicted to shift up by about 1.5−2 eV from the DFT values. This means that the value of the electron barrier is at least more than doubled with respect to those found in DFT. On the other hand, the HOMO-like states are more strongly coupled to the metal substrate than the LUMO-like states, and the perturbation approach used here to evaluate surface polarization effects may no longer be appropriate. However, because the GGA calculation already yielded a rather large lower bound for $E_F - E_H$ (3 eV), these states will not contribute to the low bias conductance.

Although the self-energy correction and surface polarization have opposite effects on the energy levels of the adsorbate orbitals, the balance of these two effects depends on the details of the molecular nature of the adsorbate and the interaction at the molecule−metal interface, which may vary from system to system. However, our results clearly indicate that it is important to go beyond a DFT treatment to obtain a realistic energy alignment at the interface, especially when considering transport properties. For example, functionalized diamondoid molecules adsorbed on the Au(111) surface were found to have a negative electron affinity from electron photoemission experiments,[32] while LDA calculations on similar systems predicted a LUMO level below the vacuum level.[33] A more realistic picture could be obtained when both the self-energy correction and screening

effects were included, in agreement with quantum Monte Carlo results.[34]

5. Conclusion

In summary, we have carried out ab initio calculations of the electronic properties of aromatic isocyanide SAMs adsorbed on the Au(111) surface. By combining many-body perturbation theory under the GW approximation and a classical image potential model, we have investigated energy level alignments at the molecule−metal interface, beyond the DFT/LDA or GGA, commonly used in the literature to study SAMs on gold. In particular, the LUMO-like states of the SAMs were found to shift upward by about 1.5−2 eV from the corresponding DFT energies, when both self-energy corrections and surface polarization effects are taken into account. In the future, additional systematic GW calculations on aromatic molecules, including benzene, are needed to establish the correct position of the LUMO level of PDI and the LUMO-like levels of the SAMs and thus determine quantitatively the upward shift compared to DFT. However, even when using the lower bound of our estimate of the LUMO-like level position ($|E_F - E_{LUMO}| \sim 2$ eV), we find a rather high barrier for electron transport for PDI SAMs. This finding is qualitatively different from that inferred from DFT results, predicting a LUMO level at near-resonance with the metal Fermi level.[12] Experimentally, there exist a wide range of measured conductance for aromatic isocyanide monolayers sandwiched between gold electrodes,[6,7,10,11] with no definitive answer about the position of the molecular HOMO and LUMO levels relative to the metal Fermi level. Our results indicate that PDI SAMs may not be very promising materials for electron transport compared to, e.g., thiolate or other SAMs.

Acknowledgment. This work was funded by NSF Grant DMR-0213618 and by DOE/BES Grant DE-FG02-06ER46262. Some of the calculations were performed at the NERSC and the SDSC facilities.

References

(1) Wang, W.; Lee, T.; Reed, M. A. *Rep. Prog. Phys.* **2005**, *68*, 523–544.

(2) Quek, S.; Venkataraman, L.; Choi, H.; Louie, S.; Hybertsen, M.; Neaton, J. *Nano Lett.* **2007**, *7*, 3477–3482.

(3) Neaton, J. B.; Hybertsen, M. S.; Louie, S. G. *Phys. Rev. Lett.* **2006**, *97*, 216405.

(4) Li, Y.; Lu, D.; Swanson, S.; Scott, J.; Galli, G. *J. Phys. Chem. C* **2008**, *112*, 6413–6421.

(5) Chen, J.; Wang, W.; Klemic, J.; Reed, M. A.; Axelrod, B. W.; Kaschak, D. M.; Rawlett, A. M.; Price, D. W.; Dirk, S. M.; Tour, J. M.; Grubisha, D. S.; Bennett, D. W. *Ann. N.Y. Acad. Sci.* **2002**, *960*, 69–99.

(6) Chen, J.; Calvet, L. C.; Reed, M. A.; Carr, D. W.; Grubisha, D. S.; Bennett, D. W. *Chem. Phys. Lett.* **1999**, *313*, 741–748.

(7) Hong, S.; Reifenberger, R.; Tian, W.; Datta, S.; Henderson, J. I.; Kubiak, C. P. *Superlattices Microstruct.* **2000**, *28*, 289–303.

(8) Dupraz, C. J.-F.; Beierlein, U.; Kotthaus, J. P. *ChemPhysChem* **2003**, *4*, 1247–1252.

(9) Lee, J.; Lientschnig, G.; Wiertz, F.; Struijk, M.; Janssen, R.; Egberink, R.; Reinhoudt, D.; Hadley, P.; Dekker, C. *Nano Lett.* **2003**, *3*, 113–117.

(10) Kim, B.; Beebe, J.; Jun, Y.; Zhu, X.-Y.; Frisbie, C. *J. Am. Chem. Soc.* **2006**, *128*, 4970–4971.

(11) Chu, C.; Ayres, J.; Stefanescu, D.; Walker, B.; Gorman, C.; Parsons, G. *J. Phys. Chem. C* **2007**, *111*, 8080–8085.

(12) Xue, Y.; Ratner, M. A. *Phys. Rev. B* **2004**, *69*, 085403.

(13) Bai, P.; Li, E.; Neerja; Collier, P. *IEEE Trans. Nanotechnol.* **2005**, *4*, 422–429.

(14) Xue, Y.; Ratner, M. A. *Phys. Rev. B* **2003**, *68*, 115406.

(15) Toher, C.; Filippetti, A.; Sanvito, S.; Burke, K. *Phys. Rev. Lett.* **2005**, *95*, 146402.

(16) Toher, C.; Sanvito, S. *Phys. Rev. Lett.* **2007**, *99*, 056801.

(17) ABINIT 5.1.2. The ABINIT code is a common project of the Université Catholique de Louvain, Corning Inc., and other contributors (URL: http://www.abinit.org).

(18) Gonze, X.; et al. *Z. Kristallogr.* **2005**, *220*, 558−562.

(19) Perdew, J. P.; Burke, K.; Ernzerhof, M. *Phys. Rev. Lett.* **1996**, *77*, 3865–3868.

(20) Godby, R. W.; Needs, R. J. *Phys. Rev. Lett.* **1989**, *62*, 1169–1172.

(21) Rozzi, C. A.; Varsano, D.; Marini, A.; Gross, E. K. U.; Rubio, A. *Phys. Rev. B* **2006**, *73*, 205119.

(22) Frisch, M. J. et al. *Gaussian 03*, revision C.02; Gaussian, Inc.: Wallingford, CT, 2004.

(23) Niehaus, T. A.; Rohlfing, M.; Sala, F. D.; Carlo, A. D.; Frauenheim, T. *Phys. Rev. A* **2005**, *71*, 022508.

(24) Herzberg, G. *Molecular Spectra and Molecular Structure: Electronic Spectra and Electronic Structure of Polyatomic Molecules*; Van Nostrand: New York, 1989; Vol. III, p 665.

(25) Burrow, P. D.; Michejda, J. A.; Jordan, K. D. *J. Chem. Phys.* **1987**, *86*, 9–24.

(26) Umari, P.; Stenuit, G.; Baroni, S. cond-mat arXiv:0811.1453, 2008.

(27) Rohlfing, M.; Louie, S. G. *Phys. Rev. B* **2000**, *62*, 4927–4944.

(28) von der Linden, W.; Horsch, P. *Phys. Rev. B* **1988**, *37*, 8351–8362.

(29) Tiago, M. L.; Chelikowsky, J. R. *Phys. Rev. B* **2006**, *73*, 205334.

(30) Eguiluz, A. G.; Hanke, W. *Phys. Rev. B* **1989**, *39*, 10433–10436.

(31) White, I. D.; Godby, R. W.; Rieger, M. M.; Needs, R. J. *Phys. Rev. Lett.* **1998**, *80*, 4265–4268.

(32) Yang, W. L. *Science* **2007**, *316*, 1460–1462.

(33) Wang, Y.; Kioupakis, E.; Lu, X.; Wegner, D.; Yamachika, R.; Dahl, J. E.; Carlson, R. M. K.; Louie, S. G.; Crommie, M. F. *Nat. Mater.* **2008**, *7*, 38–42.

(34) Drummond, N. D.; Williamson, A. J.; Needs, R. J.; Galli, G. *Phys. Rev. Lett.* **2005**, *95*, 096801.

CT800465F